SANDIA REPORT
SAND2014-1123
Unlimited Release
Printed March 2014

Band Limited Correlation Estimates for A(ξω/U) and B(ηω/U) Using Beresh et. al. 2013 Data Sets

Lawrence J. DeChant and Justin A. Smith

Prepared by
Sandia National Laboratories
Albuquerque, New Mexico 87185 and Livermore, California 94550

Sandia National Laboratories is a multi-program laboratory managed and operated by Sandia Corporation, a wholly owned subsidiary of Lockheed Martin Corporation, for the U.S. Department of Energy's National Nuclear Security Administration under contract DE-AC04-94AL85000.

Issued by Sandia National Laboratories, operated for the United States Department of Energy by Sandia Corporation.

Printed in the United States of America. This report has been reproduced directly from the best available copy.

Available to DOE and DOE contractors from
U.S. Department of Energy
Office of Scientific and Technical Information
P.O. Box 62
Oak Ridge, TN 37831

Telephone:	(865) 576-8401
Facsimile:	(865) 576-5728
E-Mail:	reports@adonis.osti.gov
Online ordering:	http://www.osti.gov/bridge

Available to the public from
U.S. Department of Commerce
National Technical Information Service
5285 Port Royal Rd.
Springfield, VA 22161

Telephone:	(800) 553-6847
Facsimile:	(703) 605-6900
E-Mail:	orders@ntis.fedworld.gov
Online order:	http://www.ntis.gov/help/ordermethods.asp?loc=7-4-0#online

SAND2014-1123
Printed March 2014

Band Limited Correlation Estimates for A(ξω/U) and B(ηω/U) Using Beresh et. al. 2013 Data Sets

Lawrence J. DeChant and Justin A. Smith
Aerosciences Department
Sandia National Laboratories
P.O. Box 5800
Albuquerque, New Mexico 87185-0825

ABSTRACT

Here we discuss an improved Corcos (Corcos (1963), (1963)) style cross spectral density utilizing zero pressure gradient, supersonic (Beresh et. al. (2013)) data sets. Using the connection between narrow band measurements with broadband cross-spectral density, i.e. $\Gamma(\xi,\eta,\omega)=\phi(\omega)A(\frac{\omega\xi}{U})B(\frac{\omega\eta}{U})\exp(-i\frac{\omega\xi}{U})$ we focus on estimating coherence expressions of the form: $A(\frac{\xi\omega_{nb}}{U})$ and $B(\frac{\eta\omega_{nb}}{U})$ where ω_{nb} denotes the narrow band frequency, i.e. the band center frequency value and ξ and η are sensors spacing in streamwise/longitudinal and cross-stream/lateral directions, respectively. A methodology to estimate the parameters which retains the Corcos exponential functional form, $A(\frac{\xi\omega}{U})=\exp(-k_{long}\frac{\xi\omega}{U})$ and $B(\frac{\eta\omega}{U})=\exp(-k_{lat}\frac{\eta\omega}{U})$ but identifies new parameters (constants) consistent with the Beresh et. al. data sets is discussed. The Corcos result requires that the data be properly explained by self-similar variable: $\frac{\xi\omega}{U}$ and $\frac{\eta\omega}{U}$. The longitudinal (streamwise) variable $\frac{\xi\omega}{U}$ tends to provide a better data collapse, while, consistent with the literature the lateral $\frac{\eta\omega}{U}$ is only successful for higher band center frequencies.

Assuming the similarity variables provide a useful description of the data, the longitudinal coherence decay constant result using the Beresh et. al. data sets yields a value for the longitudinal constant k_{long}≈0.36-0.28 that is approximately 3x larger than the “traditional” (low speed, large Reynolds number and zero pressure gradient) of k_{long}≈0.11. We suggest that the most likely reason that the Beresh et. al. data sets incur increased longitudinal decay which results in reduced coherence lengths is due to wall shear induced compression causing an adverse pressure gradient. Focusing on the higher band center frequency measurements where the frequency dependent similarity variables are applicable, the lateral or transverse coherence decay constant k_{lat}≈0.7 is consistent with the “traditional” (low speed, large Reynolds number and zero pressure gradient). It should be noted, that the longitudinal/streamwise coherence decay deviates from the value observed by other researchers while the lateral/ cross-stream value is consistent has been observed by other researchers. We believe that while the measurements used to obtain new decay constant estimates are from internal wind tunnel tests, they likely provide a useful estimate expected reentry flow behavior and are therefore recommended for use. These data could also be useful in determining the uncertainty of correlation length for a uncertainty quantification (UQ) analysis.

ACKNOWLEDGMENTS

The authors would like to thank S. Beresh, J. Henfling, R. Spiller and B. Pruett; Aeroscience Department, Sandia National Laboratories for the fundamental research that provides the basis of this analysis. Technical insight and support from S. Beresh, Aerosciences Department, R. Field, Component Science and Mechanics Department and Mikhail Mesh, Analytical Structural Dynamics Department; Sandia National Laboratories is greatly appreciated.

CONTENTS

Abstract 3

Acknowledgments 5

Introduction 11

Streamwise/Longitudinal Band Limited Correlation and Broadband Coherence Analysis A(ξω/U) 17

Lateral Band Limited Correlation and Broadband Coherence Analysis; B(ηω/U 27

Estimate for Broadband Behavior 29

Conclusions 32

References 33

APpendix: Connection Between Broadband and Narrow Band Correlation and SpectrA 35

Distribution 37

FIGURES

Figure 1. Plot of longitudinal (streamwise) band limited correlation data by Beresh et. al. in terms of variables. Black =0.41; Red =0.163; Green =0.655. Notice that first zero crossing (fξ/U) =0.25 is correctly recovered in these variables. 18

Figure 2. Plot for longitudinal (streamwise) data sets with band limited correlation in terms of variables. Black (fδ/U)=0.041, Red (fδ/U)=0.163, Green (fδ/U)=0.655. Function exp(-0.3(2π)(fξ/U) red line. 22

Figure 3. Longitudinal correlation model; (fδ/U) measurement=0.041 (0.5-2 kHz), using equation (20) α=0.6 (red) and α=0.175 (green), $(x/\delta)_0$=6 24

Figure 4. Longitudinal correlation model; (fδ/U) measurement=0.163 (2-8 kHz), using equation (20) α=0.6 (red) and α=0.175 (green), (x/δ)0=1.4 25

Figure 5. Longitudinal correlation model; (fδ/U) measurement=0.655 (8-32 kHz), using equation (20) α=0.6 (red) and α=0.175 (green), (x/δ)0=0.5 26

Figure 6. Plot for lateral (transverse) data sets with band limited correlation in terms of (fη/U)=(fy/U) variables. Black (fδ/U)=0.041, Red (fδ/U)=0.163, Green (fδ/U)=0.655. Function exp(-0.3(2π)(fη/U) red line. 28

Figure 7. Comparison between broadband longitudinal correlation R(ξ/δ) models using coherence A(C: current model: exp(-0.3ξω/U) (red); classical model (black) and Taylor hypothesis model A(ξU/U)=1(blue) compared to the data set of Wilmarth and Wooldridge 31

TABLES

Table 1: Comparison between measured streamwise dimensionless frequency band and theoretical (self-similar assumption) (fξ/U) suggesting self-similar model provides a useful model for correlation/coherence behavior. 19
Table 2. Estimate for self-similar amplitude function for longitudinal correlation/coherence using self similar variables (fξ/U) and exponential approximation: A=exp(-klongωξ/U). klong estimate (average=0.33-0.27) tends to be 3x traditional zero pressure value 21
Table 3. Damping coefficient k values assessed using best fit for empirical parameter α from "typical" low speed Bakewell data set. Notice that the average "k" value is near the literature 0.11 magnitude. 22
Table 4. Longitudinal correlation length values based upon coherence models. Experimentally measure length scale included for comparison. 32

NOMENCLATURE

Symbols

A	Streamwise/Longitudinal separable coherence function
B	Cross-stream/transverse separable coherence function
f	Ordinary frequency
H	Heaviside function
k	
L	Length scale
P	Pressure
R	Correlation function
U	Streamwise convective velocity

Greek

δ	Boundary layer thickness
η	Cross-stream spacing coordinate
Γ	Spectral density
Ψ	Phase function
ω	Angular frequency
ϕ	Frequency spectral density
ξ	Streamwise spacing coordinate
τ	Temporal spacing coordinate

Subscripts/Superscripts

c	Convection, center band
int	Integral
lat	Lateral (cross-stream)
long	Longitudinal (streamwise)
max	Maximum
min	Minimum
nb	Narrow band
pp	Pressure fluctuation

INTRODUCTION

The cross-spectral density associated with wall pressure fluctuations due to turbulent boundary layer flow is an essential component of an integrated fluid-structural modeling approach (Elishakoff (1983), Durant and Robert (1999), Tang et. al. (1995)) A very well known (used for at least 40 years) and often utilized model is that suggested by Corcos (Corcos (1963), (1963), Singer (1996)) which models the spectral density as the separable product of less complex functions as:

$$\Gamma(\xi,\eta,\omega) = A\left(\frac{\omega\xi}{U}\right)B\left(\frac{\omega\eta}{U}\right)\exp(-i\,\frac{\omega\xi}{U}) \qquad (1)$$

Here, $A\left(\frac{\omega\xi}{U}\right)$ and $B\left(\frac{\omega\eta}{U}\right)$ are real valued functions while $\exp(-i\,\frac{\omega\xi}{U})$ provides the phase behavior for the signal. Theory based arguments and measurements suggest that useful approximations to the components of equation (1) are:

$$A\left(\frac{\omega\xi}{U}\right) \approx \exp\left(-k_{long}(\frac{\omega\xi}{U})\right)$$

$$B\left(\frac{\omega\eta}{U}\right) \approx \exp\left(-k_{lat}(\frac{\omega\eta}{U})\right) \qquad (2)$$

Since these expressions represent the magnitude associated with the decomposed/separable spectral density, they can be referred to as coherence models (Singer (1996), Viazzo et. al. (2001)).

The functional form associated with equation (1) and the closure hypotheses in equation (2) remains open to interpretation and/or improvement, e.g. Singer (1996). Of even greater concern is that regardless of the functional behavior chosen the use of the self-similar independent variable $\frac{\omega\xi}{U}$ and $\frac{\omega\eta}{U}$ does not always, in particular for low frequency, provide a correct explanation of the data (Elishakoff (1983), Lowson (1967), Bull (1967)). This issue is discussed subsequently. While these expressions do have limitations, they nonetheless, provide a plausible and useful estimate for the cross-spectral density. We therefore will focus on the use of these expressions as a part of our fluid structural model and focus on identifying appropriate decay constants that better represent the flow of interest.

A large family of classical measurements (supported by more recent LES and DNS simulations) (Bull (1967), Elishakoff (1983), Viazzo et. al. (2001), Durant and Robert (1999), Lowson (1967), Wilmarth and

Yang (1970)) demonstrate that for low speed zero pressure gradient flows indicate that appropriate decay constants for the longitudinal and lateral coherences are:

$$A\left(\frac{\omega\xi}{U}\right) \approx \exp\left(-k_{long}(\frac{\omega\xi}{U})\right) \quad k_{long} \approx 0.1$$

$$B\left(\frac{\omega\eta}{U}\right) \approx \exp\left(-k_{lat}(\frac{\omega\eta}{U})\right) \quad k_{lat} \approx 0.7 \tag{3}$$

While these decay constant estimates of the coherence tend to be useful for the fundamental incompressible flat plate problem, they are nonetheless implicitly functions of a range of parameters such as Mach number, Reynolds number and flow pressure gradient. Hence, while direct application of low speed flat plate may be a useful starting point there is value in assessing decay constant behavior for flows more closely associated with the problem of interest.

Let's examine the effect of deviations from the assumptions associated with the use of equation (1). Requisite upon the use of equation (1) is that the spectral density/coherence can be represented in terms of the self-similar variable: $\frac{\omega\xi}{U}$ and $\frac{\omega\eta}{U}$. Based upon the connection between band limited correlation and the coherence functions one notes that low frequency implies large correlation lengths must be possible. As we shall see, for measurements where large correlation lengths are observed the data will be adequately modeled even for $\frac{\omega\xi}{U} << 1$.

If one can accept the use of the similarity variables as appropriate (along with the variable separation and the decay function) then one is effectively focused upon the behavior of the decay constants. Broadly, the behavior of the streamwise decay constant k_{long} is:

- Increase Reynolds number = decrease k_{long}
- Increase Mach number = decrease k_{long}
- Adverse pressure gradient = increase k_{long}
- Wall Roughness = increase k_{long}

Decay constant size is merely a model for overall correlation length of an event, in this case a wall pressure fluctuation realization. Obviously and increase in k_{long} implies a reduced correlation length. The general behavior of the decay constant is specified in Table1.

Table 1. Variation in coherence length and coherence decay constant due to flow physics.

Flow Effect	Coherence Length	Decay constant; k_{long}	Comment/Physics
Reynolds Number	Increase	Decrease	Convective transport of event dominates over diffusive behavior promoting longer correlation length; (Viazzo et. al. (2001))
Mach Number	Increase	Decrease	Turbulent fluctuation, wall shear etc. smaller for higher Mach number. k_{long} (Lowson (1967), Kistler and Chen (1962), Kraichnan.)
Adverse Pressure Gradient	Decrease	Increase	Adverse pressure gradient disrupts overall flow structure resulting in reduced coherence length. (Zawadzki et. al. (1996), Books and Hodgson (1981))
Surface Roughness	Decrease	Increase	Roughness increases diffusive like behavior; (Aupperle and Lambert (1970), Blake (1986))

To estimate the magnitude of the cross-spectral density when we have assumed the Corcos separable form and the similarity variable, we have two broad choices:

1. We can utilize the broadband Fourier transform pair that connect (measured) correlation functions to the associated spectral density (see Bull (1967), Corcos (1963) and Blake (1983))

2. There is a direct connection between narrow band (band limited) correlation measurements and the self-similar spectral densities (Smith and Lambert (1960), Wilmarth and Yang (1970), Bull (1967), Bakewell (1962), Bakewell (1963), Bakewell (1968), Clinch (1969))

We consider the broadband method first. Since we have accepted the variable separation as appropriate we concentrate on the longitudinal (streamwise) and lateral (transverse) correlations. The space time correlation can be written as:

$$R(\xi,\eta,\tau) \propto \int_{-\infty}^{\infty} \Gamma(\xi,\eta,\tau)\exp\left(i\omega\tau\right)d\omega \quad (4)$$

With an analogous Fourier transform pair (Blake (1983), Singer (1996)). The use of the proportionality implies that the transform pair definition includes the $(2\pi)^{-1}$ or $(2\pi)^{-1/2}$ term.

Let's consider the longitudinal/streamwise and lateral components of the correlation separately. The longitudinal/streamwise space time correlation is given as: $R(\xi,0,\tau) \propto \int_{-\infty}^{\infty} \Gamma(\xi,0,\tau)\exp\left(i\omega\tau\right)d\omega$ but using the Corcos expression: $\Gamma(\xi,\omega) = \phi(\omega)A(\frac{\omega\xi}{U})\exp(-i\frac{\omega\xi}{U})$ becomes:

$$R(\xi,0,\tau) \propto \int_{0}^{\infty} \phi(\omega)A(\frac{\omega\xi}{U})\cos(\omega\tau - \frac{\omega\xi}{U})d\omega \quad (5)$$

Notice that for zero time delay we can write: $R(\xi) = R(\xi,0,0) \propto \int_{0}^{\infty} \phi(\omega)A(\frac{\omega\xi}{U})\cos(\frac{\omega\xi}{U})d\omega$.

This is the similarity approximation to the longitudinal correlation. Obviously, with access to the broadband streamwise correlation we can solve the integral equation posed by equation (4) to obtain $A(\frac{\omega\xi}{U})$. The Lateral correlation follows in a similar manner where, using the Corcos closure, we find that:

$$R(\eta) = R(0,\eta,0) \propto \int_{0}^{\infty} \phi(\omega)B(\frac{\omega\eta}{U})d\omega \quad (6)$$

which provides an estimate for coherence $B(\frac{\omega\eta}{U})$.

The longitudinal correlation/coherence has an additional useful approximate connection between the autocorrelation and the streamwise correlation since Taylor's hypothesis Bull (1967), Blake (1986) suggests that streamwise space and time can be interchangeable as: ξ=Uτ. This will mean that the auto-correlation and longitudinal correlations will be effectively equivalent. Thus, from the auto-correlation pair we can write:

$$\phi(\omega) \propto \int_0^\infty R(\xi)\cos\left(\frac{\omega\xi}{U}\right)d\xi$$
$$R(\xi) \propto \int_0^\infty \phi(\omega)\cos\left(\frac{\omega\xi}{U}\right)d\omega \tag{7}$$

At this point we immediately see that there is a contradiction since we have two expressions that we can use to compute the streamwise correlation, i.e. the similarity model:

$$R(\xi) = R(\xi,0,0) \propto \int_0^\infty \phi(\omega)A(\frac{\omega\xi}{U})\cos(\frac{\omega\xi}{U})d\omega \tag{8}$$

and the Taylor hypothesis pair expressions:

$$\phi(\omega) \propto \int_0^\infty R(\xi)\cos\left(\frac{\omega\xi}{U}\right)d\xi$$
$$R(\xi) \propto \int_0^\infty \phi(\omega)\cos\left(\frac{\omega\xi}{U}\right)d\omega \tag{9}$$

By inspection the similarity hypothesis can only be consistent with the Taylor's hypothesis result for $A(\frac{\omega\xi}{U}) = 1$. Apparently, however, the two models are in good agreement even for deviations from $A(\frac{\omega\xi}{U}) = 1$ as shown by Corcos (1963), see figure 12.

The results in the discussion indicate that the broadband expressions provide a method to estimate the coherence functions the $A\left(\frac{\omega\xi}{U}\right)$ and $B\left(\frac{\omega\eta}{U}\right)$. The Beresh et. al. (2013) correlation measurements are band limited (narrow band) and do not readily support the broadband expressions. Fortunately there is an analogous theoretical framework that is applicable to the narrow band models. This approach to estimate the $A\left(\frac{\omega\xi}{U}\right)$ and $B\left(\frac{\omega\eta}{U}\right)$ self-similar coherence functions follows from a direct connection between the self similar functions and the band limited correlation: Smith and Lambert (1960), Corcos (1962), Bull (1963). By representing the kernel of the previous integral expression using a local (band limited) procedure the associated expression simplify considerably. Since the data is available in this form, these are the expression that we utilize to estimate parameter variation in the coherence models for the Beresh et. al. (2013) data sets.

STREAMWISE/LONGITUDINAL BAND LIMITED CORRELATION AND BROADBAND COHERENCE ANALYSIS A(ξω/U)

Following the derivation given in (Smith and Lambert (1960)) and (less obtainable references; reports by (Corcos (1962) and Bull and Willis (1963)) provide a derivation of the longitudinal space-time bandwidth limited correlation can be written as:

$$
\begin{aligned}
R_{nb}(\xi,\tau,f) &= \frac{|\Gamma(\xi,0,f)|}{\phi(f)}\cos(2\pi(f\tau+\frac{f\xi}{U})) \\
&= A(\frac{\xi\omega_{nb}}{U})\cos(2\pi(f\tau+\frac{f\xi}{U})) \\
&= A(2\pi\frac{\xi f}{U})\cos(2\pi(f\tau+\frac{f\xi}{U}))
\end{aligned}
\tag{10}
$$

Where we have immediately recognized that: $\frac{|\Gamma(\xi,0,f)|}{\phi(f)} = A(2\pi\frac{\xi f}{U})$ which is the Corcos coherence expression. Depending on the frequency definition we often see the form: $R_{nb}(\xi,0,f) = \frac{|\Gamma(\xi,0,f)|}{\phi(f)}\cos(2\pi(f\tau+\frac{f\xi}{U}))$. Here both "f" and ω_{nb} are the center band frequencies associated with narrow band measurement under consideration and $2\pi f = \omega$.

We note that Bull (1967) recommends: $A(\frac{\omega_{nb}\xi}{U}) \approx \exp(-0.1\frac{\omega_{nb}\xi}{U}) = \exp(-0.1\frac{0.63f\xi}{U})$ while Bakewell (1964) uses $A(\frac{f\xi}{U}) \approx \exp(-0.7\frac{f\xi}{U})$ for pipe flow, however, when we express this result in terms of angular frequency we have: $A(\frac{\omega_{nb}\xi}{U}) \approx \exp(-\frac{0.7}{2\pi}\frac{f\xi}{U}) = \exp(-0.11\frac{\omega_{nb}\xi}{U})$ Both results are associated with band limited models, however they are immediately applicable to broadband spectral density computations as well.

If the narrow band formulation suggested is indeed an appropriate model for the Beresh data sets, then when plotted in terms of self similar variable: $\frac{f\xi}{U} = (\frac{f\delta}{U})(\frac{\xi}{\delta})$ the data sets should collapse to a single curve. Here, "f" is the centerband frequency: $f \approx \frac{f_{\min} + f_{\max}}{2}$.

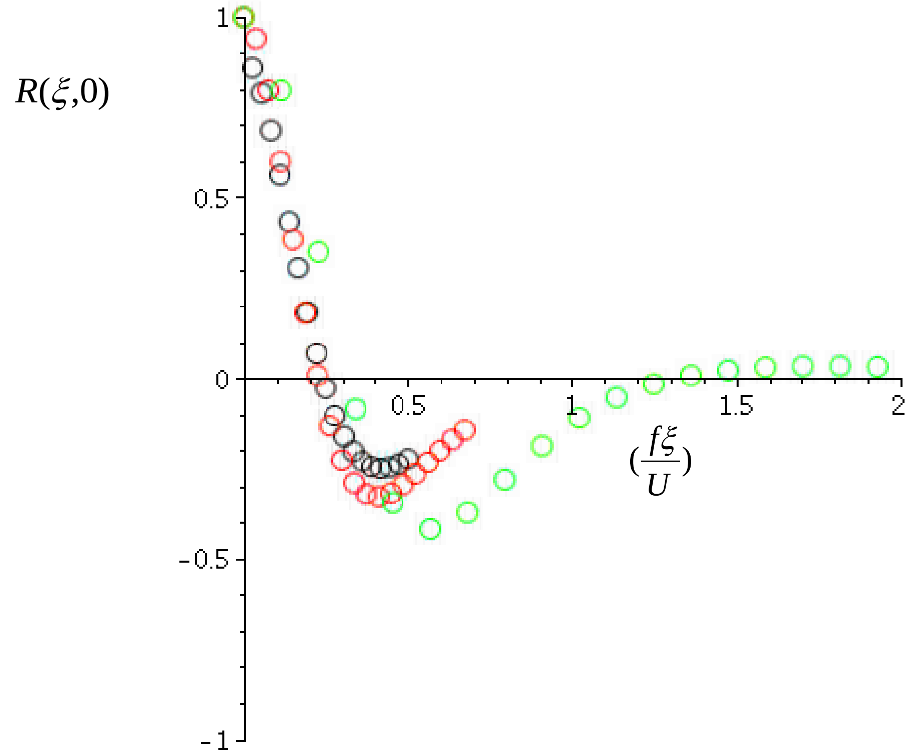

Figure 1. Plot of longitudinal (streamwise) band limited correlation data by Beresh et. al. in terms of variables. Black =0.41; Red =0.163; Green =0.655. Notice that first zero crossing (fξ/U) =0.25 is correctly recovered in these variables.

As can be seen from Figure 1. the self-similar variables partially explain the data for $(\frac{f\xi}{U}) < 1$ but are less satisfactory for larger values of $(\frac{f\xi}{U})$. Self similar models are most useful for small correlation length event. Clearly larger values of $(\frac{f\xi}{U})\Big|_{fixed}$ imply greater correlation lengths between pressure fluctuation events. Though highly correlated events over long length scales are observed in some streamwise turbulent flows as clearly demonstrated by Beresh et. al. (2013) a preponderance of events occur over shorter scales which is reflected in Figure 1.

A useful way in which to estimate the Corcos style parameters, i.e. the coefficients in $A\left(\frac{\omega\xi}{U}\right) \approx \exp\left(-k_{long}(\frac{\omega\xi}{U})\right)$ is to provide a curvefit associated in the measured $\frac{x}{\delta}$ variables which can then be related to the self similar variables in a term-by-term manner. An expression of the form:

$$R(\frac{x}{\delta}) = \exp(-\alpha\left[(\frac{x}{\delta})_0\right]^{-1}\left(\frac{x}{\delta}\right))\cos(\left(\frac{\pi}{2}\right)\left[(\frac{x}{\delta})_0\right]^{-1}\left(\frac{x}{\delta}\right)) \quad (11)$$

Where $(\frac{x}{\delta})_0$ is the first zero crossing and 0.5<α<0.7 (for the Beresh data sets) does a reasonable job in explaining the data sets. The choice of the empirical model utilized (Rubinstein and He (2002)) (this is no coincidence, of course) is consistent with our expression for the band limited correlation function. Indeed if we write the band width limited correlation function as:

$$R(\frac{\xi}{\delta}, f) = R_{nb}(\frac{\xi}{\delta},0, f) = A\left(2\pi(\frac{f\delta}{U})(\frac{\xi}{\delta})\right)\cos\left(2\pi(\frac{f\delta}{U})(\frac{\xi}{\delta})\right) \quad (12)$$

which is certainly equivalent to:

$$R(\frac{x}{\delta}, f) = R_{nb}(x,0, f) = A\left(2\pi(\frac{f\delta}{U})(\frac{x}{\delta})\right)\cos\left(2\pi(\frac{f\delta}{U})(\frac{x}{\delta})\right) \quad (13)$$

Comparing equation (11) and (13) it is immediately apparent that: $\cos\left(2\pi(\frac{f\delta}{U})(\frac{x}{\delta})\right) = \cos(\frac{\pi}{2}\left[(\frac{x}{\delta})_0\right]^{-1}(\frac{x}{\delta}))$ or:

$$2\pi(\frac{f\delta}{U})(\frac{x}{\delta}) = \frac{\pi}{2}\left[(\frac{x}{\delta})_0\right]^{-1}(\frac{x}{\delta}) \to (\frac{f\delta}{U}) = \frac{1}{4}\left[(\frac{x}{\delta})_0\right]^{-1} \quad (14)$$

We estimate the same result for the other frequency bands in table 1.

Table 1: Comparison between measured streamwise dimensionless frequency band and theoretical (self-similar assumption) (fξ/U) suggesting self-similar model provides a useful model for correlation/coherence behavior.

Dimensionless center band $(\frac{f\delta}{U})$ **measurement**	Zero crossing $(\frac{x}{\delta})_0$	Theoretical dimensionless center band $\left[4(\frac{x}{\delta})_0\right]^{-1}$	Relative error (%) |meas-theor|/meas.
0.041	6.0	$[(4)(6)]^{-1}$=0.042	3 %
0.163	1.4	$[(4)(1.3)]^{-1}$=0.178	9%
0.655	0.5	$[(4)(0.5)]^{-1}$=0.5	23 %

These results are certainly encouraging in that they suggest that the self similar variables support the data sets as indicated by Figure 1. They also suggest that that the band limited expressions are providing a far better description of the measurements as compared to the broadband method.

We can gain further confidence by examining other available data sets, for example, Bakewell (1964) and Clinch (1969) both low speed data sets. Both researchers present the correlation model as:

$$R(\xi, f) = A\left(2\pi(\frac{f\xi}{U})\right)\cos\left(2\pi(\frac{f\xi}{U})\right) \tag{15}$$

They do not provide sufficient information to plot using the $2\pi(\frac{f\delta}{U})(\frac{\xi}{\delta})$ variable. Nonetheless we can readily compare values for the first zero crossing. Both Bakewell and Clinch show that the measured value for the first zero crossing is $(\frac{f\xi}{U})\Big|_0 = 0.25$ which is precisely consistent with our model since (Note the location of the zero crossing in Figure 1):

$$2\pi(\frac{f\xi}{U})\Big|_0 = \frac{\pi}{2}\left[(\frac{x}{\delta})_0\right]^{-1}(\frac{x}{\delta})_0 \rightarrow (\frac{f\delta}{U})\Big|_0 = \frac{1}{4} \tag{16}$$

Obviously their measurements also support the efficacy of the similarity variable $\frac{f\xi}{U}$ and the use of the narrow band procedure.

This success suggests that we should be able to estimate the magnitude expression as well. Indeed, using our previous result we have $A\left(\frac{\omega x}{U_c}\right) = A\left(2\pi(\frac{f\delta}{U})(\frac{U}{U_c})(\frac{x}{\delta})\right)$ where we assume it takes the exponential form estimated implying that: $\exp\left(-k_{long}(\frac{\omega x}{U_c})\right) = \exp\left(-k_{long}(\frac{\omega\delta}{U})(\frac{U}{U_c})(\frac{x}{\delta})\right)$. Notice that we have included the effect of the free stream to convective velocity ratio where $(\frac{U}{U_c}) \approx 1.0 - 1.7$ We can now equate this result to our empirical model $\exp(-\alpha\left[(\frac{x}{\delta})_0\right]^{-1}\left(\frac{x}{\delta}\right))$ whereby:

$$k_{long} = \frac{\alpha\left[(\frac{x}{\delta})_0\right]^{-1}}{2\pi(\frac{f\delta}{U})(\frac{U}{U_c})} \qquad (17)$$

As was done previously we can estimate the "k_{long}" constant in the Corcos result using Beresh's supersonic data. Here we include the effect of the convective velocity which varies as: $(\frac{U}{U_c}) \approx 1-1.33$.

Table 2. Estimate for self-similar amplitude function for longitudinal correlation/coherence using self similar variables (fξ/U) and exponential approximation: A=exp(-klongωξ/U). klong estimate (average=0.33-0.27) tends to be 3x traditional zero pressure value

Dimensionless center band $(\frac{f\delta}{U})$ **measurement**	Zero crossing $(\frac{x}{\delta})_0$	Corcos style $A = \exp\left(-k_{long}\frac{\omega\xi}{U}\right)$; $k_{long} = \frac{-\alpha\left[(\frac{x}{\delta})_0\right]^{-1}}{2\pi(\frac{f\delta}{U})(\frac{U}{U_c})}$,α=0.6
0.041	6.0	k=0.39-0.3 (U/U_c=1-1.33)
0.163	1.4	k=0.42-0.31
0.655	0.5	k=0.29-0.22

Examination of these results suggest that they are three times as large other reported results where k_{long} is typically k_{long}=0.11 results. To get a better sense of how these parameters represent the actual data we plot the results against the data sets in Figure 2.

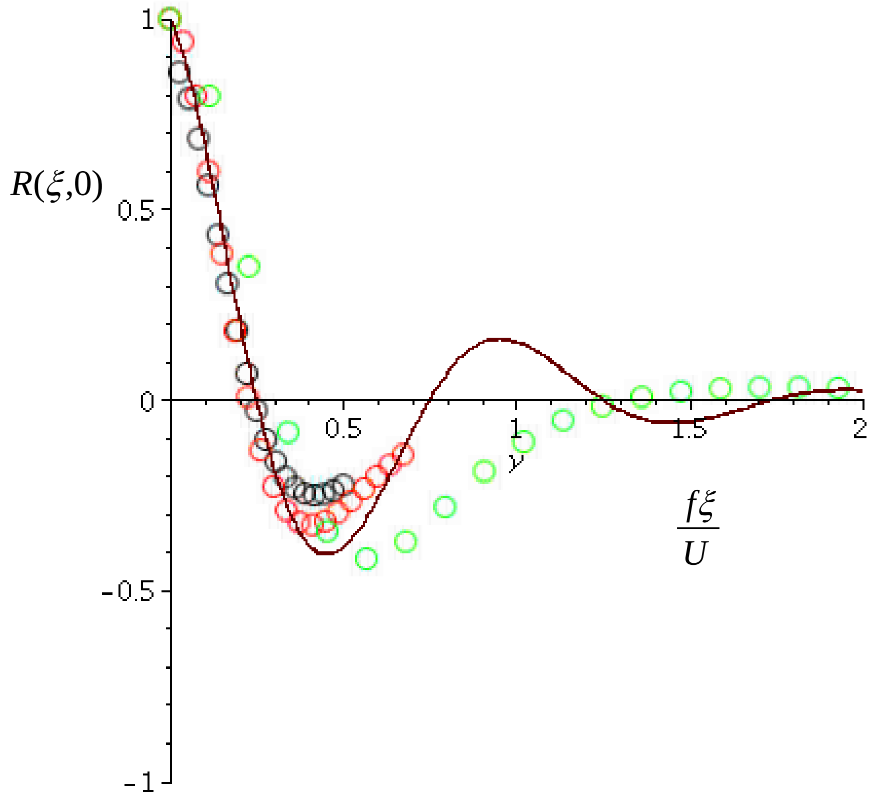

Figure 2. Plot for longitudinal (streamwise) data sets with band limited correlation in terms of variables. Black (fδ/U)=0.041, Red (fδ/U)=0.163, Green (fδ/U)=0.655. Function exp(-0.3(2π)(fξ/U) red line.

Obviously this discrepancy in k_{long} is concerning since we cannot determine if the Beresh data themselves are the source or is there an issue with the reduction procedure. If we utilize our curve fit procedure we see that the best fit from our empirical model for α was α≈0.6. Fortunately, the Bakewell (1964) expression permit us to make a direct estimate for α. Bakewell represents the A function as $A(\frac{f\xi}{U}) \approx \exp(-0.7\frac{f\xi}{U})$. So by equating exponential arguments we have:

$$-0.7(\frac{fx}{U}) = -\alpha\left[(\frac{x}{\delta})_0\right]^{-1}(\frac{x}{\delta}) \tag{19}$$

Using $(\frac{fx}{U})\Big|_0 = 0.25$ for $(\frac{x}{\delta}) = (\frac{x}{\delta})_0$ we find that $\alpha_{bake} = 0.7(0.25) = 0.175$. Using this value we can estimate the "k_{long}" value in table 3

Table 3. Damping coefficient k values assessed using best fit for empirical parameter α from "typical" low speed Bakewell data set. Notice that the average "k" value is near the literature 0.11 magnitude.

Corcos style $A = \exp\left(-k\frac{\omega\xi}{U}\right)$; $k = \frac{-\alpha\left[(\frac{x}{\delta})_0\right]^{-1}}{2\pi(\frac{f\delta}{U})(\frac{U}{U_c})}$,**α=0.175**
k=0.11-0.087 (U/U_c=1-1.33)
k=0.12-0.09
k=0.084-0.06

Clearly using $\alpha=\alpha_{Bake}=0.175$ yields k values that are much more consistent with typical (low speed, high Reynolds number, zero pressure gradient) measurements.

To see that the chosen value for α is consistent with the Beresh data we present plots of the actual data using

$$R(\frac{x}{\delta}) = \exp(-\alpha\left[(\frac{x}{\delta})_0\right]^{-1}\left(\frac{x}{\delta}\right))\cos(\left(\frac{\pi}{2}\right)\left[(\frac{x}{\delta})_0\right]^{-1}\left(\frac{x}{\delta}\right)) \quad (20)$$

in Figures 3.-5.

For both α=0.6 (red) and α=0.175 (green) for the three center band frequencies. Clearly, α=0.6 and k≈0.37 fits the Beresh far better than α=0.175 and k=0.1.

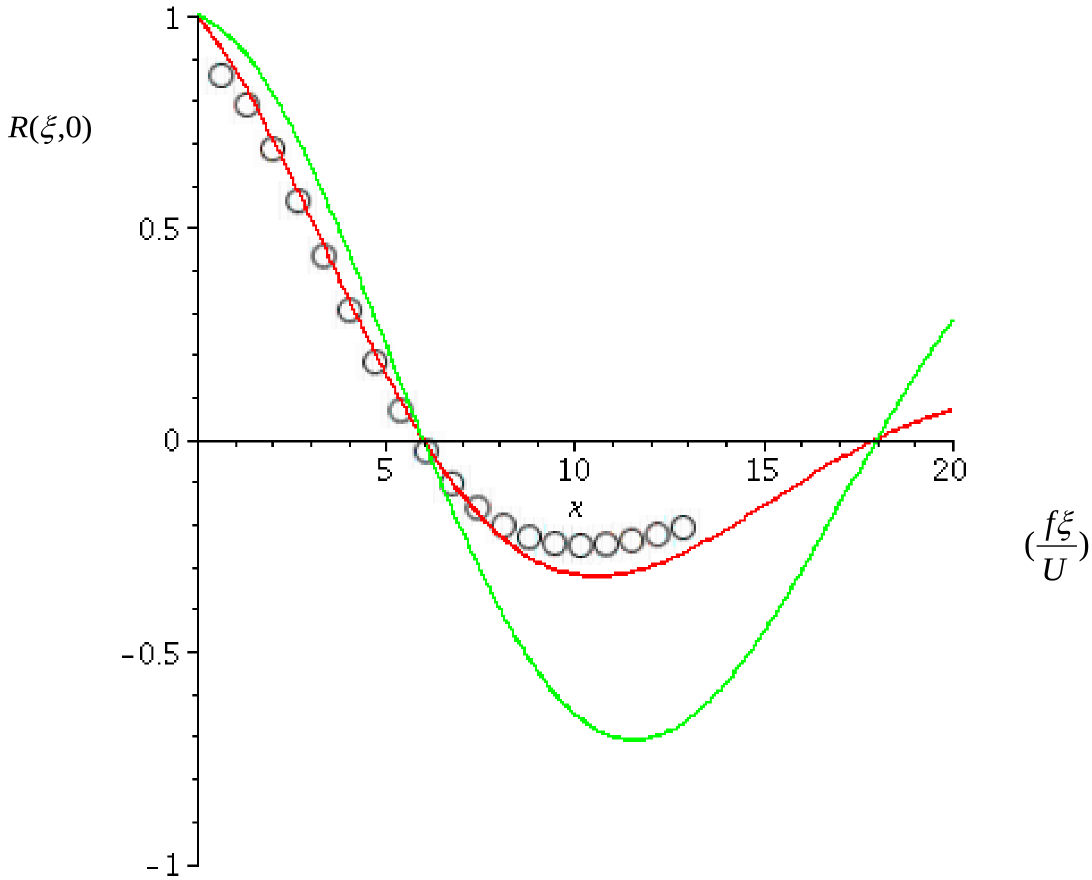

Figure 3. Longitudinal correlation model; (fδ/U) measurement=0.041 (0.5-2 kHz), using equation (20) α=0.6 (red) and α=0.175 (green), $(x/\delta)_0=6$

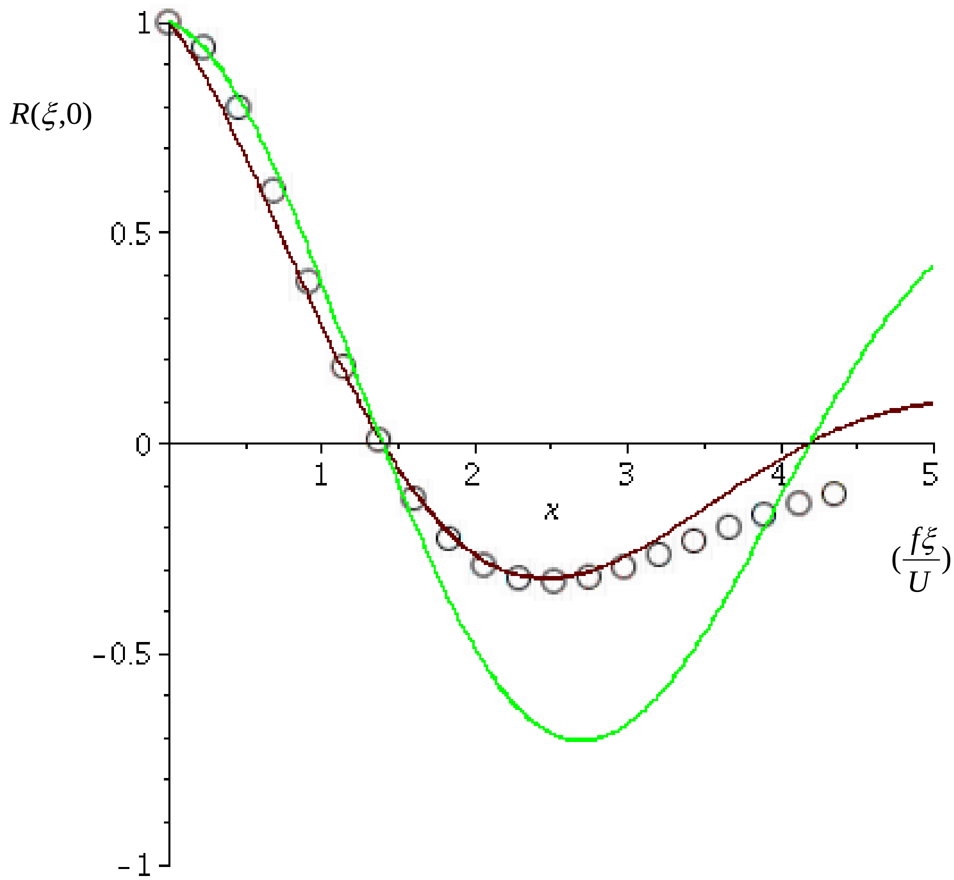

Figure 4. Longitudinal correlation model; (fδ/U) measurement=0.163 (2-8 kHz), using equation (20) α=0.6 (red) and α=0.175 (green), (x/δ)0=1.4

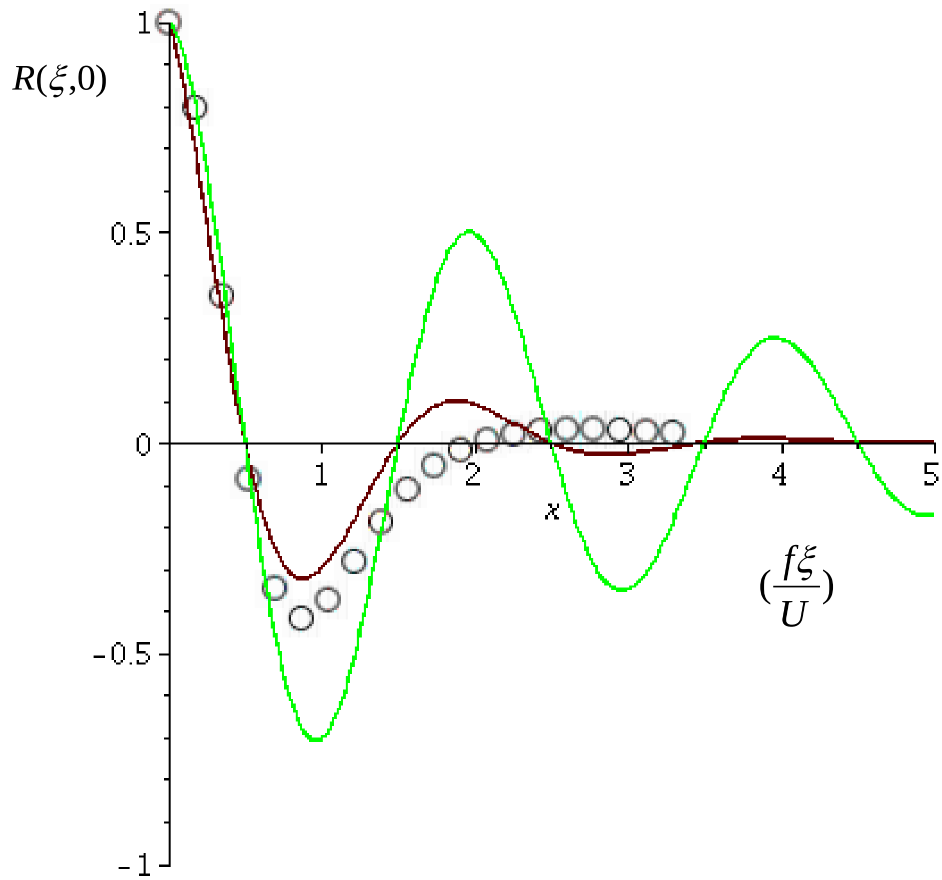

Figure 5. Longitudinal correlation model; (fδ/U) measurement=0.655 (8-32 kHz), using equation (20) α=0.6 (red) and α=0.175 (green), (x/δ)0=0.5

Following this discussion we conclude that the longitudinal data sets measured by Beresh et. al. (2013) are moderately well explained by the narrow band models which provide direct access to the coherence expression that compose the Corcos broadband spectral density functions. The decay coefficients estimated for the longitudinal coherence are significantly larger, 2-3 times, than the "classical" large Reynolds number, low Mach number, zero pressure gradient values in the literature. We suggest that a possible reason for this behavior is a small adverse pressure gradient associated with compression shocks. Unfortunately, theory-based models to estimate correlation based behavior are not readily available which make a direct connection pressure correlation to flow field physical behavior difficult.

LATERAL BAND LIMITED CORRELATION AND BROADBAND COHERENCE ANALYSIS; B(ηω/U

Here we provide estimates for the decay constant associated with the lateral narrow band correlation and the associated broad band lateral coherence function $B(\frac{\xi\omega_{nb}}{U})$. Unlike the (narrow band) streamwise correlation where a sinusoidal term is included, the lateral correlation is a strictly exponential decay type expression. As such, matching data is relatively straightforward since the lateral (transverse) correlation is traditionally modeled by an exponential decay term only. Assuming (and here this will NOT be a good assumption for all frequency bands) that the transverse/lateral correlation can be represented in terms of the similarity variable: $\frac{f\eta}{U} = \frac{fy}{U} = \left(\frac{f\delta}{U}\right)\frac{y}{\delta}$ we can write:

$$R(\frac{y}{\delta}) = \exp(-k_{lat}\left(\frac{f\delta}{U}\right)\frac{y}{\delta}) \qquad (21)$$

Where $\left(\frac{f\delta}{U}\right)$ is represented by the frequency bands: 0.041, 0.0163 and 0.655 which follow from the streamwise correlation/coherence discussion. Since there is no sinusoidal term and no zero crossing to "anchor" a model, it makes most sense to simply plot the lateral correlation in terms of the similarity variable and then asses a best fit for k_{lat}.

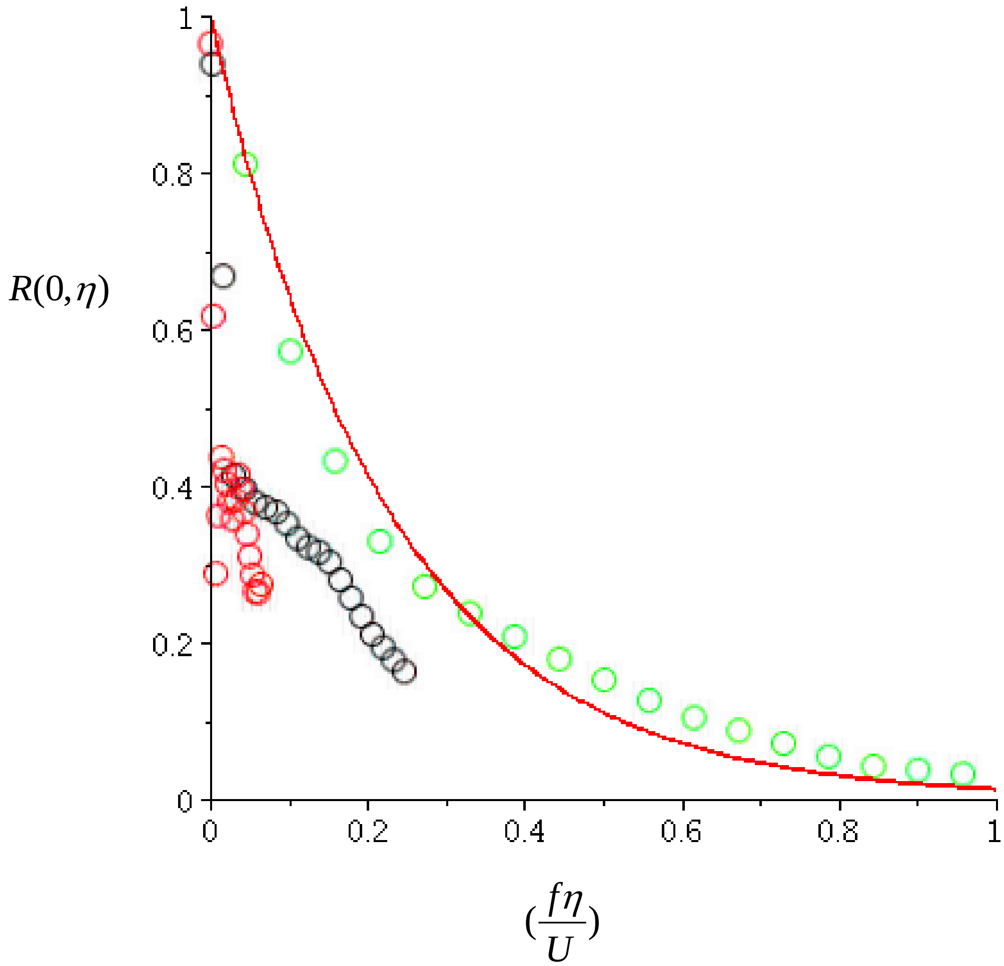

Figure 6. Plot for lateral (transverse) data sets with band limited correlation in terms of (fη/U)=(fy/U) variables. Black (fδ/U)=0.041, Red (fδ/U)=0.163, Green (fδ/U)=0.655. Function exp(-0.3(2π)(fη/U) red line.

Examination of the figure suggest the use of the similarity variable $(\frac{f\eta}{U})$ is not justified for the lateral correlation since the use of this independent variable fails to coalesce the Beresh measurements into a single curve as was accomplished for $(\frac{f\xi}{U})$ in the streamwise problem. For an explanation of the potential reason for this failure we note that low frequency band limited correlations are not well modeled via the use of the similarity variables $(\frac{f\xi}{U})$. Lowson (1967) indicates that $(\frac{f\delta}{U}) < 2.7$ that the use of the self-similar variable $(\frac{f\xi}{U})$ is not appropriate since a very large correlation length would be requisite. Elishakoff suggest a similar bound in terms of displacement thickness as: $(\frac{f\delta^*}{U}) < 0.2$ However inspection of our data suggests the use of the $(\frac{f\xi}{U})$ is useful for $(\frac{f\delta}{U}) = 0.041$ for the streamwise disturbances. This statement is consistent with the Beresh et. al. discussion where large coherent streamwise structures are noted in their investigation. Since they do not identify equivalent structures in the lateral direction, it is perhaps of little surprise that attempts to correlate lateral disturbances with $(\frac{f\eta}{U})$ are unsuccessful.

ESTIMATE FOR BROADBAND BEHAVIOR

While narrow band correlation data sets measured by Beresh et. al. were utilized to estimate the coherence functions $A(\frac{\xi\omega_{nb}}{U})$ and $B(\frac{\xi\omega_{nb}}{U})$ we are actually more interested in these coherence expressions in a broadband framework. The connection between coherence models is effectively trivial, i.e.:

$$\begin{aligned} A(\frac{\xi\omega_{nb}}{U}) &\rightarrow A(\frac{\xi\omega}{U}) \\ B(\frac{\eta\omega_{nb}}{U}) &\rightarrow B(\frac{\eta\omega}{U}) \end{aligned} \tag{22}$$

As discussed previously, we can directly compare the correlation closure expressions and their associated decay constants to those utilized by other researchers, but in addition we can use the narrow band derived coherence models within the broadband correlation definitions and compare directly to known broadband correlation measurements. This type of comparison was performed by Bull (1967).

Focusing on the longitudinal broadband correlation we recall that via the transform pair and the Corcos style spectral density we derived equation (8): $R(\xi) = R(\xi,0,0) \propto \int_0^\infty \phi(\omega) A(\frac{\omega\xi}{U}) \cos(\frac{\omega\xi}{U}) d\omega$ and from the Taylor hypothesis: $R(\xi) \propto \int_0^\infty \phi(\omega) \cos\left(\frac{\omega\xi}{U}\right) d\omega$. We emphasize that R(ξ) is the broadband spatial correlation and is distinctly different than its narrow band counterpart.

To compute a broadband correlation, we need, of course access to the frequency spectrum φ(ω). While many semi-empirical models are available, see Hwang et. al. (2000) it is perhaps most appropriate to utilize the dedicated frequency spectral density model suggested by DeChant and Smith (2013) which takes the form:

$$\begin{aligned}\Phi_{pp}(\omega) &= \frac{\delta}{U}\left|p'\right|^2\left[\frac{\pi\delta_0^3\omega}{(1+\omega^2)(\alpha^2\omega^2+\delta_0^2)^2}+\beta\exp(-\sqrt{\frac{\alpha}{\delta_0}\kappa_0\omega})\right] \\ &= \frac{\delta}{U}(4\tau_w)^2\left[\frac{\pi\delta_0^3\omega}{(1+\omega^2)(\alpha^2\omega^2+\delta_0^2)^2}+\beta\exp(-\sqrt{\frac{\alpha}{\delta_0}\kappa_0\omega})\right]\end{aligned} \tag{23}$$

where α, β, κ_0 and δ_0 are constants discussed in the reference and are not notations used in this document.

Using the integral expressions in figure 7, we estimate the broadband longitudinal correlation R(ξ) using the result obtained here: $A(\frac{\xi\omega_{nb}}{U}) \rightarrow A(\frac{\xi\omega}{U}) = \exp(-0.3\frac{\xi\omega}{U})$ and compare to the data set of Wilmarth and Wooldridge (1962). In addition we compare with the more classical result: $A(\frac{\xi\omega}{U}) = \exp(-0.11\frac{\xi\omega}{U})$ and Taylor hypothesis expression (effectively $A(\frac{\xi\omega}{U}) \equiv 1$):

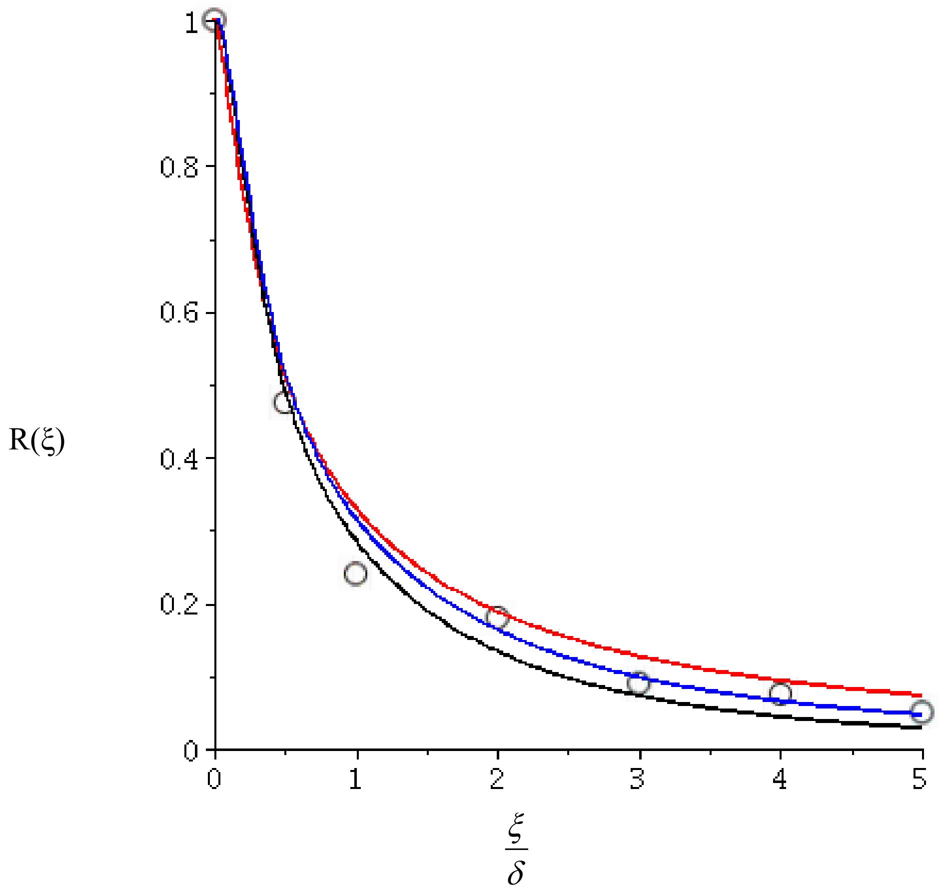

Figure 7. Comparison between broadband longitudinal correlation R(ξ/δ) models using coherence A(C: current model: exp(-0.3ξω/U) (red); classical model (black) and Taylor hypothesis model A(ξU/U)=1(blue) compared to the data set of Wilmarth and Wooldridge

Inspection of Figure 7. Suggests that while the classical model with a coherence decay constant 0.1 matches the correlation measurements of Wilmarth and Wooldridge (1962) "best" ; both the local approximation with decay constant 0.3 and the Taylor hypothesis approximation are in reasonable agreement as well. Therefore, the use of the dedicated model $\exp(-0.3\frac{\xi\omega}{U})$ for reentry applications is recommended. We note that in a counter intuitive manner, that the larger decay constant associated with $\exp(-0.3\frac{\xi\omega}{U})$ yields a correlation that decays more slowly than the other models.

A useful (and perhaps surprising) result can be obtained by computing the formal integral lengths associated with the broadband correlation functions computed previously. The integral length scale follows as:

$$L_{\text{int}} = \int_0^\infty R(\xi) d\xi = \int_0^\infty \int_0^\infty \phi(\omega) A(\frac{\omega\xi}{U}) \cos(\frac{\omega\xi}{U}) d\omega d\xi \qquad (24)$$

Consider the longitudinal correlation lengths $\frac{L_{\text{int}}}{\delta}$ associated with the coherence models:

Table 4. Longitudinal correlation length values based upon coherence models. Experimentally measure length scale included for comparison.

Coherence Model	$\frac{L_{\text{int}}}{\delta}$
$A(\frac{\xi\omega}{U}) = \exp(-0.3\frac{\xi\omega}{U})$	2.76
$A(\frac{\xi\omega}{U}) = \exp(-0.1\frac{\xi\omega}{U})$	1.88
$A(\frac{\xi\omega}{U}) = 1$	1.35
Palumbo (2012)	0.8-4.3
Beresh et. al. (2013)	0.5-6.0

CONCLUSIONS

The major task associated with the spatial correlation project is to compute an improved Corcos style cross spectral density utilizing dedicated Beresh et. al. data sets. This effectively means estimating coherence expressions of the form: $A(\frac{\xi\omega_{nb}}{U})$ and $B(\frac{\xi\omega_{nb}}{U})$. Here we have connected narrow band measurements to the broadband cross-spectral density, i.e. $\Gamma(\xi,\eta,\omega) = \phi(\omega) A(\frac{\omega\xi}{U}) B(\frac{\omega\eta}{U}) \exp(-i\frac{\omega\xi}{U})$. A methodology to estimate the parameters which retains the Corcos exponential functional form, $A(\frac{\xi\omega}{U}) = \exp(-k_{long}\frac{\xi\omega}{U})$ and $B(\frac{\eta\omega}{U}) = \exp(-k_{lat}\frac{\eta\omega}{U})$ but identifies new parameters (constants) consistent with the Beresh et. al. (2013) data sets has been discussed. The longitudinal result for the coherence decay constant using the Beresh data sets suggests a value for the longitudinal constant k_{long}≈0.36-0.28 that is approximately 3x larger than the "traditional" (low speed, large Reynolds number and zero pressure gradient) of k_{long}≈0.11.

Recalling that, broadly the behavior of the streamwise decay constant k_{long} is affected by:

- Increase Reynolds number = decrease k_{long} (Viazzo et. al. (2001))
- Increase Mach number = decrease k_{long} (Lowson (1967), Kistler and Chen (1962), Kraichnan.)
- Adverse pressure gradient = increase k_{long} (Zawadzki et. al. (1996), Books and Hodgson (1981))
- Wall Roughness = increase k_{long} (Aupperle and Lambert (1970), Blake (1986))

We postulated that a possible reason that the Beresh data sets incur increased longitudinal decay, i.e. reduced coherence lengths is due to wall shear induced compression causing an adverse pressure gradient. The lateral or transverse coherence decay constant $k_{lat}\approx 0.7$ is consistent with the "traditional" (low speed, large Reynolds number and zero pressure gradient). We believe that while the measurements used to obtain new decay constant estimates are from internal wind tunnel tests and that they provide a useful estimate expected reentry flow behavior and are therefore recommended for use.

REFERENCES

1. Aupperle, F. A., Lambert, R. F., "Effect of Surface Roughness on Measured Wall Pressure Fluctuations Beneath a Turbulent Boundary Layer," Journal of the acoustical Soc. of Am., pp. 359-370, 1970.
2. Bakewell, H. P., Carey, G. F., Libuha, J. J., Schloemer, H. H., Von Winkle, W. A., Wall Pressure Correlations in Turbulent Pipe Flow, USL report 559, 1962, http://www.dtic.mil/cgi-bin/GetTRDoc?AD=AD0283683
3. Bakewell, H. P. "Longitudinal Space-Time Correlation Function in Turbulent Airflow," Journ. Acoust. Soc. Of Am., V. 36, pp. 146-148 (1964).
4. Bakewell, H. P., "Narrow-Band Investigations of the Longitudinal Space-Time Correlation Function in Turbulent Airflow, Journ. Acoust. Soc. Of Am., V. 35, pp. 936-937 (1963).
5. Beresh, S. J., Henfling, J. S., Spiller, R. W., Pruett, B. O., "Very-Large-Scale Coherent Structures in the Wall Pressure Field Beneath a Supersonic Turbulent Boundary Layer," Physics of Fluids, 25, 9, September, pp. 095104-095104-19, (2013).

6. Blake, W. K. Mechanics of Flow-Induced Sound and Vibration, V. 1-2, Academic Press, NY, 1986.
7. Brooks, T. F., Hodgson, T. H., "Trailing Edge Noise Prediction from Measured Surface Pressures", Journal of Sound and Vibration, 78, pp. 69-117, 1981.
8. Bull, M. K., "Wall Pressure Fluctuations Associated with Subsonic Turbulent Boundary Layer Flow," JFM, 28, pp. 719-754, 1967.
9. Bull, M. K., Willis, J. L., "Some Results of Experimental Investigations of the Surface Pressure Field Due to a Turbulent Boundary layer," U. of South Hampton, AASU Report 199, 1-27, 1962.
10. Clinch, J. M. "Measurement of the Wall Pressure Field at the Surface of a Smooth-Walled Pipe Containing Turbulent Water Flow," Journal of Sound and Vibration, 9, pp. 398-419, (1969)
11. Corcos, G. M., "Pressure Fluctuations in Shear Flows,", University of California Institute of Engineering Report Series, 183, 2.
12. Corcos, G. M., "Resolution of Pressure in Turbulence," J. Acoustical Society of America, V. 35, 2, pp. 192-199, 1963.
13. Corcos, G.M. The Structure of the Turbulent Pressure Field in Boundary Layer Flows, JFM, 18, pp. 353-378. 1963.
14. DeChant, L., Smith, J., "An Approximate Turbulent Pressure Fluctuation Frequency Spectra for a Finite Supersonic Plate," draft manuscript completed, contact ljdecha@sandia.gov 2013.
15. Durant, C., Robert, G., Vibro-Acoustic Response of a Pipe Excited by a Turbulent Internal Flow, Flow, Turbulence and Combustion, 61: pp. 55-69, 1963.
16. Elishakoff, I, *Probabilistic Theory of Structures*, Dover, Mineoloa NY, 1983.
17. Hwang , Y. F., Bonness, W. K., Hambric, S. A., "Comparison of semi-empirical models for turbulent boundary layer wall pressure spectra," *Journal of Sound and Vibration* 319, 199–217, 2009
18. Kistler, A. L., Chen, W. S., "the Fluctuating Pressure Field in a Supersonic Turbulent Boundary Layer," JFM, JFM, 16, pp. 41-64, 1963.
19. Lowson, M. V., "Prediction of Boundary Layer Pressure Fluctuations,", TR AFFDL-TR-67-167 (1967); http://www.dtic.mil/cgi-bin/GetTRDoc?AD=AD0832715
20. Palumbo, D. "Determining Correlation and Coherence Lengths in Turbulent Boundary Layer Flight Fields," Journal of Sound and Vibration, 331 3721-3737.
21. Rubinstein, H. and He, G. The Eulerian Time Domain Correlation Function in Homogeneous Isotropic Turbulence, ICASE report (2002) www.cs.odu.edu/~mln/ltrs-pdfs/icase-2002-2.pdf

22. Singer, B. A., "Turbulent Wall-Pressure Fluctuations: New Model for Off-Axis Cross-Spectral Density, NASA CR 198297, 1996.

23. Smith, M. W., Lambert, R. F., "Propagation of Band Limited Noise,", Journal of the Acoustic Soc. Of Am., V 32, 4, pp. 512-514.

24. Tang, Y., Silcox, R., and Robinson, J., Modeling of Sound Transmission Through Shell Structures With Turbulent Boundary Layer Excitation, AIAA paper 98-1760.

25. Viazzo, S., Dejoan, A., Schiestel, R., Spectral Features of the Wall-Pressure Fluctuations in Turbulent Wall Flows with and without Perturbations Using LES, Heat and Fluid Flow, 22, pp. 39-52, 2001.

26. W. Wilmarth, W. and Woolridge, C. E. "Measurements of the Fluctuating Pressure at the Wall Beneath a Thick Turbulent Boundary Layer," *J. Fluid. Mech*. 14, 187, 1962.

27. Wilmarth, W. W. and Yang, C. S., "Wall-Pressure Fluctuations Beneath Turbulent Boundary Layers on a Flat Plate and a Cylinder, JFM, 41, pp47-80, 1970.

28. Zawadzkii, I, Gershfeld, J. L., Wang, M., "Hydroacoustic Forcing Function Modeling Using DNS Database, Center for Turbulence research, Summer Program, 1996, www.ctr.stanford.edu/ctrsp96/zawadzk

APPENDIX: CONNECTION BETWEEN BROADBAND AND NARROW BAND CORRELATION AND SPECTRA

Let's examine the band limited autocorrelation and auto spectrum (auto spectral density). Consider first the definition for broadband autocorrelation as:

$$R_{pp}(\tau) = \lim_{t\to\infty} \frac{1}{t}\int_0^t p(t)p(t+\tau)dt = \langle p(t)p(t+\tau)\rangle \quad \text{(A.1)}$$

Notice that equation (1) is simply a time based average of signals over a long time period. If we assume that signals are ergodic, then a correlation based on an ensemble average is equivalent. The spectral density and the auto correlation are related through the transform pair as:

$$\begin{aligned} \phi(\omega) &\propto \int_0^\infty R_{pp}(\tau)\cos(\omega\tau)d\tau \\ R_{pp}(\tau) &\propto \int_0^\infty \phi(\omega)\cos(\omega\tau)d\omega \end{aligned} \quad \text{(A.2)}$$

Let's now consider the effect where the signals are band limited over a $\Delta\omega$. Now, the raw input signal has been filtered such that the output signal is:

$$p(t,\Delta\omega) \propto \int_0^\infty p(\omega)\cos(\omega t)H(\omega)d\omega \qquad \text{(A.3)}$$

Where $H(\omega)$ is frequency response of the filter and is usually a Heaviside expression over $\omega_c - \frac{\Delta\omega}{2} < \omega < \omega_c + \frac{\Delta\omega}{2}$ where ω_c is the centerband frequency of the filter. Using an ensemble average motivation, we can write the band limited auto correlation as:

$$R(\tau,\Delta\omega) = \langle p(t,\Delta\omega)\, p(t+\tau,\Delta\omega)\rangle = \int_0^\infty \phi(\omega)\cos(\omega t)(H(\omega))^2 d\omega \qquad \text{(A.4)}$$

The mean square amplitude of $p(t,\Delta\omega)$ can be written:

$$\left|p^2(t,\Delta\omega)\right| \propto \int_0^\infty \phi(\omega)(H(\omega))^2 d\omega \qquad \text{(A.5)}$$

But over a small frequency band we have:

$$\left|p^2(t,\Delta\omega)\right| \approx \phi(\omega)\Delta\omega \qquad \text{(A.6)}$$

Thus, the full integral can be evaluated as:

$$R(\tau,\Delta\omega) = \langle p(t,\Delta\omega)\, p(t+\tau,\Delta\omega)\rangle = \phi(\omega)\Delta\omega\cos(\omega\tau - \psi(\omega)) \qquad \text{(A.7)}$$

Where $\psi(\omega)$ is the phase information for this signal. Thus, by an appropriate definition for the autocorrelation magnitude, we arrive at the connection auto correlation and frequency spectrum that does not involve integration over all frequency space.

DISTRIBUTION

1	MS0346	Richard Field	1526 (electronic copy)
1	MS0346	Mikhail Mesh	1523 (electronic copy)
1	MS0825	Steven Beresh	1515 (electronic copy)
1	MS0825	Lawrence DeChant	1515 (electronic copy)
1	MS0825	Jeff Payne	1515 (electronic copy)
1	MS0825	Justin Smith	1515 (electronic copy)
1	MS9018	Central Technical Files	8944 (electronic copy)
1	MS0899	Technical Library	4536 (electronic copy)

Sandia National Laboratories